Type III Secretion System Translocon Component EseB Forms Filaments on and Mediates Autoaggregation of and Biofilm Formation by *Edwardsiella tarda*

Zhi Peng Gao,[a,b,c] Pin Nie,[a] Jin Fang Lu,[a,c] Lu Yi Liu,[a] Tiao Yi Xiao,[b] Wei Liu,[a] Jia Shou Liu,[a] Hai Xia Xie[a]

State Key Laboratory of Freshwater Ecology and Biotechnology, Institute of Hydrobiology, Chinese Academy of Sciences, Wuhan, Hubei Province, China[a]; College of Animal Science and Technology, Hunan Agricultural University, Changsha, Hunan Province, China[b]; University of Chinese Academy of Sciences, Beijing, China[c]

The type III secretion system (T3SS) of *Edwardsiella tarda* plays an important role in infection by translocating effector proteins into host cells. EseB, a component required for effector translocation, is reported to mediate autoaggregation of *E. tarda*. In this study, we demonstrate that EseB forms filamentous appendages on the surface of *E. tarda* and is required for biofilm formation by *E. tarda* in Dulbecco's modified Eagle's medium (DMEM). Biofilm formation by *E. tarda* in DMEM does not require FlhB, an essential component for assembling flagella. Dynamic analysis of EseB filament formation, autoaggregation, and biofilm formation shows that the formation of EseB filaments occurs prior to autoaggregation and biofilm formation. The addition of an EseB antibody to *E. tarda* cultures before bacterial autoaggregation prevents autoaggregation and biofilm formation in a dose-dependent manner, whereas the addition of the EseB antibody to *E. tarda* cultures in which biofilm is already formed does not destroy the biofilm. Therefore, EseB filament-mediated bacterial cell-cell interaction is a prerequisite for autoaggregation and biofilm formation.

Edwardsiella tarda is a Gram-negative bacterium with a wide range of hosts, including fish and humans. *E. tarda* causes hemorrhagic septicemia in fish and gastrointestinal and extraintestinal infections in humans (1–3). The type III secretion system (T3SS) of *E. tarda* plays a pivotal role in infection and enables the bacteria to survive and replicate in phagocytes and epithelial cells (4–7).

The bacterial T3SS nanomachine, delivering effector proteins directly from the bacterial cytosol to host cells (8, 9), consists of three parts: the basal body, needle, and translocation pore (10). The gene cluster of the T3SS in *E. tarda* contains 34 genes, which encode secretion apparatus, chaperones, translocators, effectors, and regulators (5, 11). The *esrA-esrB* (5) and *esrC* (12) genes in the T3SS gene cluster together with *phoP-phoQ* (13) and *phoB-phoR* (14) outside the T3SS gene cluster control the virulence of *E. tarda*. Deletion of *esrB* abolished the secretion of the translocon proteins EseB, EseC, and EseD (5), which can form a protein complex after secretion (5, 15, 16). Mutation of *eseB* led to an *E. tarda* replication defect in host cells (5). EseB is required not only for translocating effectors into host cells (11) but also for bacterial autoaggregation in a T3SS-inducing medium, Dulbecco's modified Eagle's medium (DMEM) (5).

EseB is homologous to EspA of enteropathogenic *Escherichia coli* (EPEC) or enterohemorrhagic *Escherichia coli* (EHEC), and it has been reported that EspA forms a sheath-like structure on the bacterial surface, as revealed by immunofluorescent staining and immunogold labeling, and is required for effector translocation (17–19). EspA of EPEC or EHEC also functions as an adhesin in microcolony formation on epithelial cells and is involved in bacterial aggregation during biofilm formation on abiotic surfaces or salad leaves (19, 20). The contribution of the T3SS to biofilm formation has also been reported for other bacteria. For instance, the T3SS of the phytopathogen *Xanthomonas citri* subsp. *citri* is necessary for biofilm formation (21), and hyperactivity of the T3SS encoded by *Salmonella* pathogenicity island 1 (SPI1) can me-

diate biofilm-like cell aggregation (22). Biofilms, highly structured microbial communities featuring bacterial cells attaching to a biotic or abiotic surface and embedded in a matrix (23, 24), may neutralize the conventional antimicrobial effect and host defense and thus are difficult to eradicate (25). Hence, identification of proteins involved in biofilm formation by bacterial pathogens may provide information for antibiofilm treatment (26, 27).

In the present study, we investigated the role of EseB in the formation of filamentous appendages on the surface of *E. tarda*, and we proved that EseB filament-mediated bacterial cell-cell interaction is a prerequisite for autoaggregation and biofilm formation.

MATERIALS AND METHODS

Bacterial strains and plasmids. The bacterial strains and plasmids used in this study are listed in Table 1. *E. tarda* strains (28) were grown in tryptic soy broth (TSB; BD, MD, USA) or on tryptic soy agar (TSA; BD) at 28°C, and *Escherichia coli* strains were cultured in Luria-Bertani (LB) broth (BD) or on LB agar at 37°C. For the induction of T3SS proteins, *E. tarda* strains were cultured in DMEM (Life Technologies, NY, USA) at 25°C under a 5% (vol/vol) CO_2 atmosphere. When required, the medium was supplemented with appropriate antibiotics at the following concentra-

TABLE 1 Strains and plasmids used in this study

Strain or plasmid	Description[a]	Reference or source
Strains		
E. tarda		
PPD130/91	Wild type; Km^s Col^r Amp^s	28
Δ*eseB*	PPD130/91 with in-frame deletion of *eseB*	15
Δ*flhB*	PPD130/91 with in-frame deletion of *flhB*	7
Δ*eseB*/pJN105-*eseB*	Δ*eseB* with pJN105-*eseB*	This study
E. coli		
DH5α	α complementation	TaKaRa
BL21(DE3)	*E. coli* B F$^-$ *ompT hsdS*(r$_B$$^-$ m$_B$$^-$) *dcm*$^+$ Tet^r *gal* (DE3) *endA* Hte	Novagen
Plasmids		
pMD18-T	Cloning vector, Amp^r	TaKaRa
pJN105	Arabinose-inducible gene expression vector; *araC*-P$_{BAD}$; Gm^r	29
pJN105-*eseB*	pJN105 with wild-type *eseB*	This study
pET-28b	Cloning vector; Km^r	Novagen
pET-28b-*eseB*	pET-28b with *eseB*	This study
pFPV25.1	Derivative of pBR322 with *gfpmut3A* under the control of the constitutive promoter	30

[a] Km, kanamycin; Col, colistin; Amp, ampicillin; Gm, gentamicin. Superscript r and s indicate resistance and sensitivity, respectively.

tions: 12.5 μg/ml colistin (Col; Sigma, St. Louis, MO, USA), 100 μg/ml ampicillin (Amp; Sigma), and 100 μg/ml gentamicin (Gm; Sigma).

Complementation of a mutant strain. The *eseB* gene and its ribosome binding site were amplified with the genomic DNA of *E. tarda* PPD130/91 as the template and ligated into the EcoRI and XbaI sites of pJN105 (29) to produce plasmid pJN105-*eseB*, which was transformed into the Δ*eseB* strain. The primers used are listed in Table 2. EseB expression was induced in the Δ*eseB*/pJN105-*eseB* strain when the culture was supplemented with 50 mM L-arabinose (Biosharp, Anhui, China).

EseB protein expression, purification, and antibody preparation. The *eseB* gene was cloned into a modified pET-28b vector with a SUMO (small ubiquitin-related modifier) protein fused at the N terminus after the His$_6$ tag, and the recombinant plasmid was transformed into *E. coli* BL21(DE3) cells induced with 0.1 mM isopropyl-β-D-thiogalactopyranoside (IPTG) (Sigma, USA) at 20°C for 16 h. Harvested cells were lysed by sonication in lysis buffer (400 mM NaCl, 50 mM Tris-HCl [pH 8.0], and 10% glycerol). Cell lysates were centrifuged at 18,000 × *g* for 1 h at 4°C, and the supernatant was incubated with Ni beads (GE Healthcare) at 4°C for 3 h. The beads were then washed with lysis buffer before elution with 250 mM imidazole. Purified His$_6$-SUMO-EseB was digested with a ubiquitin-like protease (ULP1), and flowed through a HiTrap Q HP column to separate His$_6$-SUMO from EseB. Purified EseB protein was kindly provided by ZhiXiong Zeng at Huazhong Agricultural University.

Purified EseB was adjusted to 1.0 μg/μl or 0.8 μg/μl in phosphate-buffered saline (PBS) (200 mM NaCl, 25 mM Tris-HCl [pH 7.9]). To prepare EseB antibody, eight 6-week-old naive C57BL/6 mice were immunized individually with 200 μl EseB and adjuvant each time. For the first immunization, equal volumes of EseB (1.0 μg/μl) and Freund's complete adjuvant (Sigma) were mixed and injected into mice subcutaneously in the abdomen. Two weeks later, equal volumes of EseB (1.0 μg/μl) and

Freund's incomplete adjuvant (Sigma) were mixed and injected into mice intraperitoneally. For the third and fourth immunizations, equal volumes of EseB (0.8 μg/μl) and Freund's incomplete adjuvant were mixed and injected into mice intraperitoneally. Two weeks after the final immunization, blood was collected to isolate EseB antiserum. The antisera were then pooled before being used. Six-week-old C57BL/6 mice were purchased from Vital River Laboratory Animal Technology Co. (Beijing) and cultured at the Experimental Animal Centre, Wuhan Institute of Virology, Chinese Academy of Sciences. The animal study proposal was approved by the Institutional Animal Care and Use Committee (IACUC) of the Experimental Animal Centre, Wuhan Institute of Virology, Chinese Academy of Sciences.

Autoaggregation assay. Fresh colonies of *E. tarda* strains were inoculated into 5 ml DMEM and cultured at 25°C under a 5% CO$_2$ atmosphere. Twenty-four hours later, the culture was subcultured at a 1:200 dilution in DMEM. To evaluate autoaggregation, the culture supernatants were carefully transferred to determine optical density at 540 nm (OD$_{540}$) values every 2 h until 40 h postsubculture (hps). Meanwhile, images of *E. tarda* autoaggregation in glass tubes were acquired with a camera at 24 hps. Moreover, *E. tarda* cells that autoaggregated on coverslips were photographed under a Hitachi S-4800 field emission scanning electron microscope (Hitachi, Japan).

Scanning electron microscopy (SEM). Bacteria that settled on coverslips were fixed in 2.5% glutaraldehyde (Sigma) in PBS for 4 h at room temperature prior to washes with PBS. The samples were then dehydrated with a series of gradient acetone, 10%, 30%, 50%, 70%, 90%, 100%, and 100%, with 15 min for each dehydration step, before being freeze-dried. Subsequently, samples were coated with gold film by sputter coating before being observed under a field emission scanning electron microscope (S-4800; Hitachi, Japan).

Immuno-transmission electron microscopy. For immuno-transmission electron microscopy (immuno-TEM) experiments, bacteria were grown in DMEM for 20 h, grids were then immersed in the culture, and the culture was allowed to grow for another 4 h. The grids with settled bacteria were fixed and blocked with 10% BSA (bovine serum albumin) (Sigma) in PBS for 30 min before being stained with anti-EseB antibody at a 1:200 dilution for 2 h and protein A-coated colloidal gold particles conjugated to donkey anti-mouse antibody (10 nm; Sigma) at a 1:100 dilution. Colloidal gold particle-coated samples were air dried and negatively stained with 1% phosphotungstic acid before being examined under a transmission electron microscope (HT-7700; Hitachi, Japan). Protein A binds specifically to the Fc part of the IgG molecule (donkey anti-mouse

TABLE 2 Oligonucleotides used in this study

Primer	Nucleotide sequence
pET-*eseB*-for	AGAATTCATGACTGTCAATACAGACTACC
pET-*eseB*-rev	AAAGCTTGCGGATATTCTGGGCGATGG
pJN105-for	TCTGTAACAAAGCGGGACCAAAG
pJN105-rev	GTGCTGCAAGGCGATTAAGTTGG
eseB-com-pJN105-for	ATGGATCCAACGCACTTTTCCGCCCTTGG
eseB-com-pJN105-rev	TTTCTAGATTACTAGCGGATATTCTGGGCG ATGGATT

antibody), and colloidal gold particles were coated with protein A; thus, the filamentous appendages composed of EseB are labeled with electron-dense colloidal gold particles.

Immunofluorescence microscopy. Bacteria were subcultured at a 1:200 dilution in DMEM in a 24-well plate with embedded coverslips. Bacteria that settled on the coverslips were fixed in 4% paraformaldehyde (PFA) in PBS and labeled by immunofluorescence staining. Briefly, the bacteria were blocked with 10% BSA in PBS prior to antibody treatment. Antibodies were used at the following dilutions: mouse anti-EseB polyclonal antibody was used at 1:200, and donkey anti-mouse IgG (Alexa 488; Molecular Probes, USA) was used at 1:200. Images were photographed with a confocal laser scanning microscope (NOL-LSM 710; Carl Zeiss, Germany).

Biofilm formation assay. *E. tarda* strains were subcultured in 24-well tissue culture plates with embedded coverslips. At 8 h, 18 h, 24 h, and 36 h postsubculture, the culture supernatants were removed carefully, and the coverslips were gently rinsed three times with PBS prior to fixation with 2.5% glutaraldehyde. The slides were then processed for SEM observation.

Effect of EseB antibody on autoaggregation and biofilm formation. Wild-type *E. tarda* cells expressing green fluorescent protein (GFP) from pFPV25.1 (30) were subcultured at a 1:200 dilution in DMEM and incubated for 15 h, and anti-EseB antibody (2.65 mg/ml) was then added at a 1:2,000, 1:1,000, 1:200, 1:100, or 1:50 dilution. Nine hours later, autoaggregation was recorded by taking images of turbidity in glass tubes before the determination of the OD_{540} values of the culture supernatants. In parallel, *E. tarda* cells grown in 24-well plates with embedded coverslips were treated with EseB antibody at the dilutions indicated above, and EseB filaments that developed on the bacteria were labeled by immunofluorescence staining.

To learn whether EseB antibody influenced the well-developed biofilm or not, *E. tarda* wild-type cultures were supplemented at 24 hps with EseB antibody at 1:2,000, 1:1,000, 1:200, 1:100, and 1:50 dilutions. At 4 h postsupplementation, the culture supernatants were carefully aspirated, and the remaining biofilms were rinsed twice with prewarmed PBS before being fixed in 4% PFA and stained with 1% crystal violet. Biofilms stained with crystal violet were photographed before being solubilized with 200 μl of a 1% SDS solution to determine the OD_{630} by using an ELx800 microplate reader (BioTek, USA).

Motility assay. To measure motility, *E. tarda* strains were subcultured at a 1:40 dilution in TSB at 28°C, and at 3 hps, similar amounts of each strain were spotted onto fresh TSA plates containing 0.4% agar. Twelve hours later, the motility of *E. tarda* strains was assessed by comparing the diameters of motility halos on soft agar.

Statistical analysis. All data are expressed as means ± standard deviations (SD) of data from three independent experiments and were analyzed statistically by using Student's *t* test, with *P* values of <0.05 being considered significant.

RESULTS

Dynamic analysis of *E. tarda* autoaggregation. Autoaggregation of *E. tarda* was abolished by insertion mutation of *eseB* when bacteria were grown in DMEM for 24 h (5). To analyze the dynamics of autoaggregation, *E. tarda* wild-type strain PPD130/91, its isogenic Δ*eseB* mutant, and the complemented Δ*eseB* strain (Δ*eseB*/pJN105-*eseB* strain) were subcultured at 1:200 in DMEM. The OD_{540} of the culture supernatant was measured at intervals of 2 h until 40 hps. At 22 hps, the OD_{540} value of the culture supernatant from the *E. tarda* wild-type and Δ*eseB*/pJN105-*eseB* strains was lower than that of the Δ*eseB* strain (Fig. 1A), indicating that autoaggregation started at 20 hps. At 24 hps, most wild-type and Δ*eseB*/pJN105-*eseB* cells settled to the bottom of the glass tubes, and their supernatants became transparent, whereas the culture of the Δ*eseB* strain remained cloudy (Fig. 1B), demonstrating that

deletion of *eseB* abolishes the autoaggregation of *E. tarda* in DMEM.

At 24 hps, bacteria that settled on the coverslips in a 24-well plate in DMEM were fixed for examination by SEM. Bacterial clumps were observed for the wild-type and the Δ*eseB*/pJN105-*eseB* strains but not the Δ*eseB* strain. In contrast to the wild-type strain, a few sparsely distributed bacteria were observed for the Δ*eseB* strain (Fig. 1C).

EseB forms filamentous appendages. EseB (GenBank accession number AAX76903.1) shares 21% identity and 35% similarity with EspA of EPEC (accession number WP_000380757.1), 35% identity and 51% similarity with HrpA of *Pseudomonas syringae* (accession number AAB00126.1), and 29% identity and 46% similarity with SseB of *Salmonella enterica* (accession number WP_001611818.1). Both EspA and HrpA can form filamentous appendages on the bacterial surface (31, 32). To test if EseB forms a filamentous appendage(s) on the bacterial surface, we used high-magnification SEM to observe bacteria. As shown in Fig. 2A, filamentous appendages were observed on the surface of *E. tarda* wild-type cells but not on the surface of cells of the Δ*eseB* strain, and the filamentous appendages attached *E. tarda* wild-type cells to the glass coverslip or connected one *E. tarda* cell to another (Fig. 2A). By immuno-TEM, EseB proteins labeled with gold particles were observed to be distributed along the filamentous appendages on the surface of *E. tarda* wild-type cells (Fig. 2B). By immunofluorescence staining, EseB was found to form filamentous appendages on the surface of *E. tarda* wild-type cells under a confocal microscope (Fig. 2C). No filamentous appendage was observed on the surface of cells of the Δ*eseB* strain (Fig. 2). Taken together, these results demonstrate that EseB forms filamentous appendages on the surface of *E. tarda* wild-type cells.

EseB is required for biofilm formation by *E. tarda* in DMEM. We tested if EseB is involved in biofilm formation when *E. tarda* is grown in DMEM. *E. tarda* strains were grown in DMEM for 24 h under static conditions. The culture supernatants were carefully aspirated, and the remaining biofilms were rinsed twice with prewarmed PBS before being fixed with 4% PFA and stained with 1% crystal violet. As shown in Fig. 3A, the wild-type strain formed biofilm, while the Δ*eseB* mutant strain did not. Interestingly, a flagellum-null Δ*flhB* mutant strain of *E. tarda* was able to form biofilm, and quantification analysis showed that biofilm formation by the Δ*flhB* strain was not significantly different from that by the wild type (Fig. 3A), even though deletion of *flhB* abolished the mobility of *E. tarda* on soft TSA (Fig. 3B). These results demonstrate that EseB, but not flagella, is required for biofilm formation by *E. tarda* in DMEM.

Dynamics of EseB filaments and biofilm development. As EseB forms filaments and is required for biofilm formation, we investigated the role of EseB filaments in biofilm development. By SEM, we noticed that diffused *E. tarda* cells were observed at 8 hps, and EseB filaments were found to attach *E. tarda* cells to the abiotic glass coverslip. At 18 hps, *E. tarda* began to autoaggregate, and EseB filaments helped to connect *E. tarda* cells together. At 24 hps, EseB filaments weaved a robust web-like structure to maintain the *E. tarda* macrocolony. At 36 hps, the developed biofilm was similar to that at 24 hps (Fig. 4). Together with data from the dynamic analysis of autoaggregation, these data indicate that EseB forms filaments on the bacterial surface, EseB filaments attach bacteria to abiotic surfaces, and growing EseB filaments connect bacterial
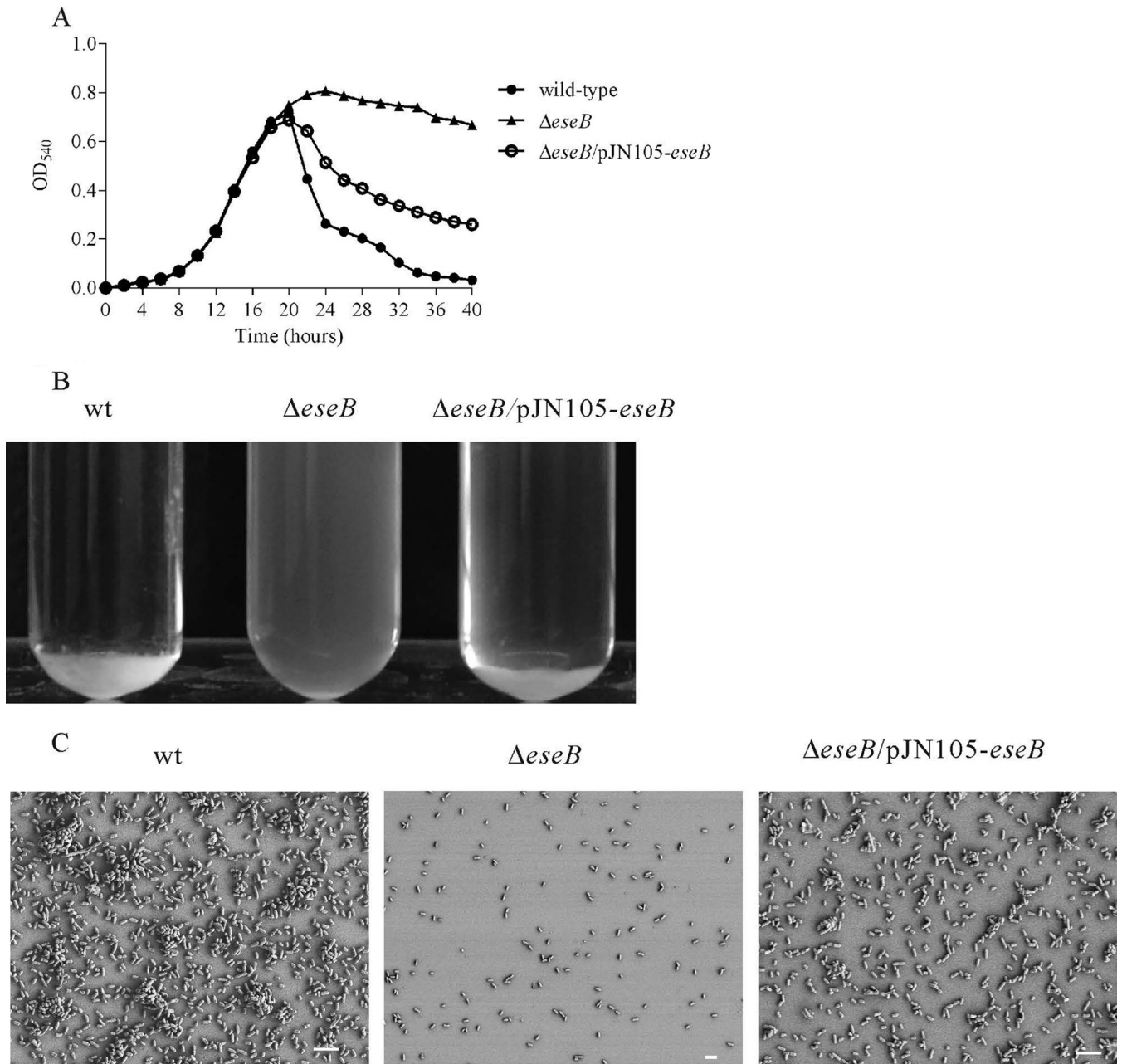
FIG 1 Dynamic analysis of *E. tarda* autoaggregation. (A) EseB-mediated *E. tarda* autoaggregation. Deletion of *eseB* abolished *E. tarda* autoaggregation, and expression of *eseB* in pJN105-*eseB* induced by 50 mM L-arabinose restored autoaggregation to wild-type levels. (B) Autoaggregation of wild-type (wt), Δ*eseB*, and Δ*eseB*/pJN105-*eseB* cells in DMEM at 25°C. The wild-type and the complementing strains began to autoaggregate at 20 hps. (C) Autoaggregation observed by SEM. Cell clumps that settled on coverslips were observed for the wild-type and Δ*eseB*/pJN105-*eseB* strains but not the Δ*eseB* strain. Bars, 4 μm.

cells, thus causing autoaggregation of and formation of biofilm by *E. tarda* in DMEM.

EseB antibody blocks *E. tarda* autoaggregation and biofilm formation by affecting EseB filaments. To test if the EseB filament-mediated connections among bacterial cells are crucial for autoaggregation and biofilm formation, we examined the effect of EseB antibody on autoaggregation and biofilm formation. EseB antibody was added to the *E. tarda* wild-type culture at 1:2,000, 1:1,000, 1:200, 1:100, and 1:50 dilutions, and at 15 h and 9 h post-supplementation, the turbidity of the *E. tarda* culture in glass tubes was measured. The culture supernatants were carefully transferred to evaluate their OD$_{540}$ values. As shown in Fig. 5A, the autoaggregation of *E. tarda* wild-type cells was inversely proportional to the amount of EseB antibody added; the culture treated with EseB antibody at 1:100 and at 1:50 dilutions had no significant difference in turbidity, as revealed by OD$_{540}$ values, which indicates that EseB antibody supplementation at a 1:100 dilution completely blocks autoaggregation of *E. tarda* wild-type cells (Fig. 5A). The biofilms that developed with the addition of EseB antibody were stained with crystal violet, and the absorbance of dis-
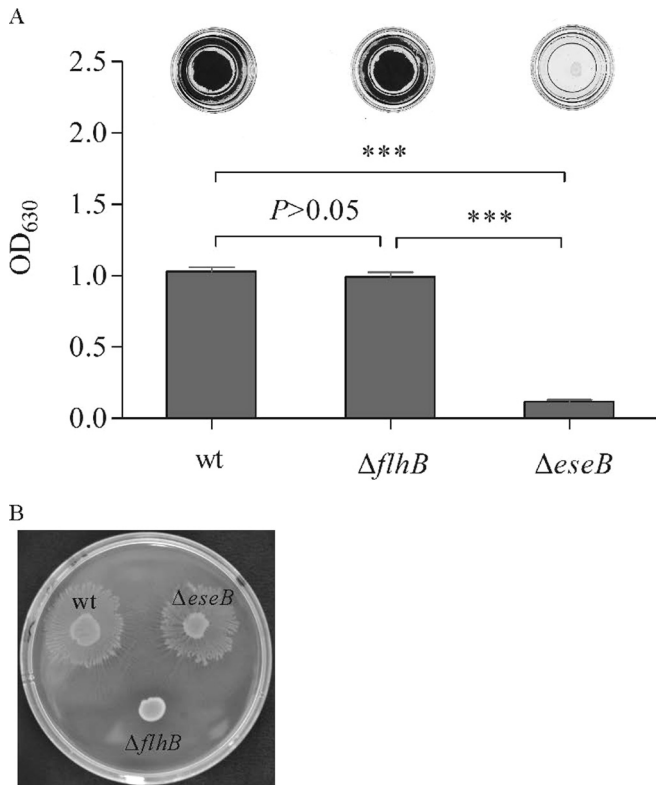
A

wt

$\Delta eseB$

B

wt

$\Delta eseB$

C

wt

$\Delta eseB$

A

B
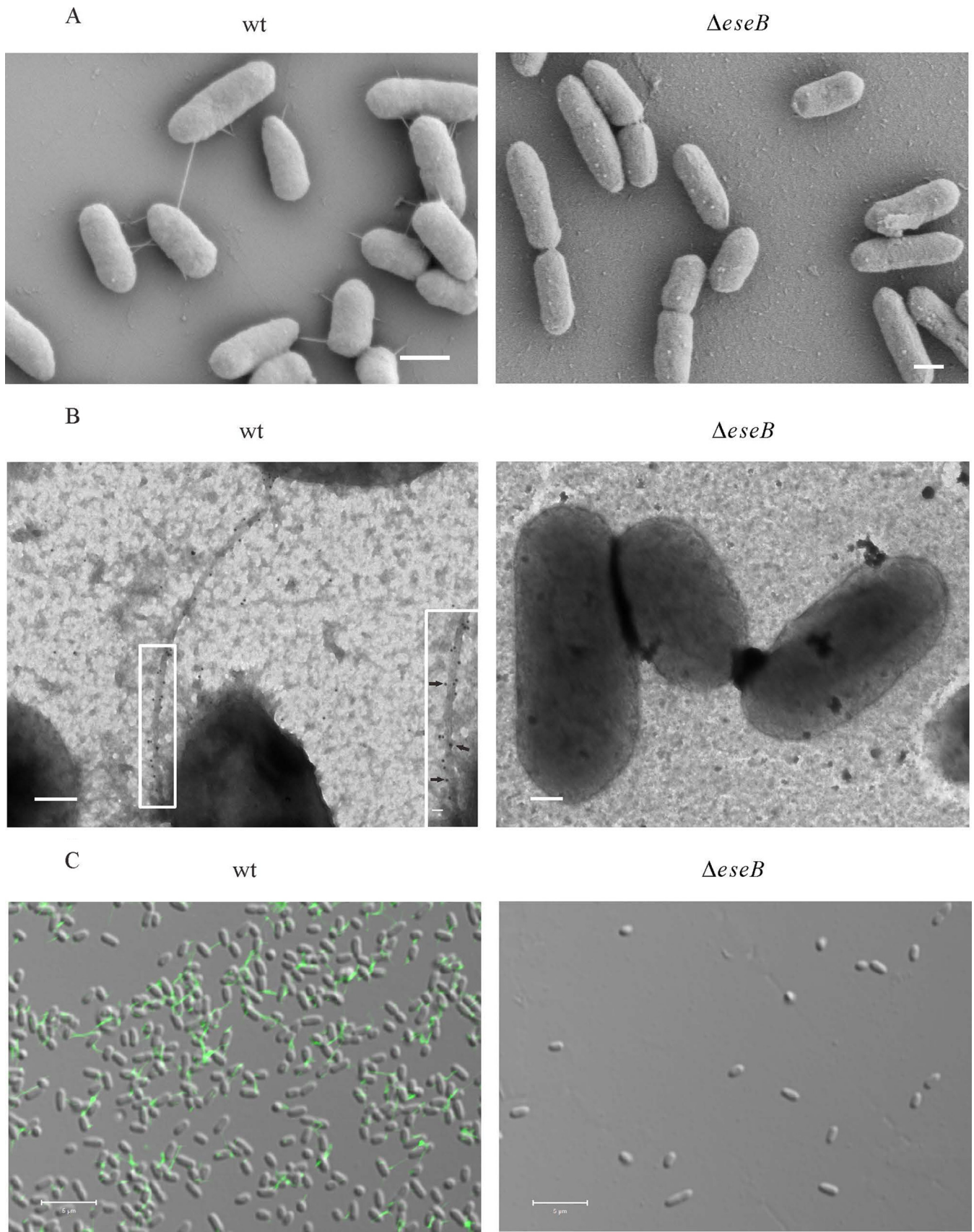
FIG 3 EseB but not FlhB is involved in *E. tarda* biofilm formation in DMEM. (A) Deletion of *flhB* does not influence *E. tarda* biofilm formation in DMEM. Biofilms that developed were stained with crystal violet, and biofilm formation was evaluated by examining the OD$_{630}$ of the dissolved crystal violet. *** indicates a significant difference at a *P* value of <0.001. (B) Motility of wild-type, Δ*eseB*, and Δ*flhB* cells on TSA with 0.4% agar. Images of motility halos were taken 12 h after loading of bacteria.

solved crystal violet at 630 nm was determined. As shown in Fig. 5B, the amount of biofilm that developed was inversely proportional to the amount of EseB antibody added. Again, no difference in biofilm formation at two concentrations (1:100 and 1:50) of EseB antibody was observed, in agreement with the effect of EseB antibody on autoaggregation. To analyze the effect of EseB antibody on EseB filaments, *E. tarda* wild-type cells expressing GFP from plasmid pFPV25.1 were grown for 15 h in a 24-well plate with embedded coverslips and treated with EseB antibody at different dilutions for 9 h. Coverslips were washed with PBS and then fixed with PFA before immunofluorescence labeling with EseB antibody. As shown in Fig. 5C, when EseB antibody was added at a 1:2,000 dilution, there were fewer filamentous appendages on the surface of *E. tarda* wild-type cells than on wild-type cells treated with naïve mouse serum (labeled as untreated). Interestingly, with the increase in the amount of EseB antibody added, the EseB signal detected on the surface of *E. tarda* wild-type cells became weaker. This result indicates that EseB which was secreted to

assemble filamentous appendages on the *E. tarda* surface before bacterial autoaggregation and biofilm formation might be neutralized by EseB antibody.

Next, we tested if the EseB antibody has any effect on mature *E. tarda* biofilms. The EseB antibody was added at 1:2,000, 1:1,000, 1:200, 1:100, and 1:50 dilutions to *E. tarda* wild-type cultures at 24 hps, a time point at which mature biofilm had already formed (Fig. 3). At 4 h post-antibody supplementation, the remaining biofilms were stained with crystal violet. The crystal violet was dissolved for measuring the OD$_{630}$ to evaluate the remaining biofilms. As shown in Fig. 5D, EseB antibody did not destroy the mature biofilm, as the biofilms did not change with increasing EseB antibody concentrations. Collectively, these data demonstrate that the EseB antibody blocks autoaggregation and biofilm formation but has no effect on biofilms that have already formed.

DISCUSSION

Tan et al. hypothesized that EseB of *E. tarda* may be a component of an extracellular filamentous organelle or appendage based on the requirement for EseB for *E. tarda* autoaggregation in DMEM (5). Here, we show that EseB can indeed form filamentous appendages on the surface of *E. tarda* and is involved in autoaggregation and biofilm formation through EseB filament-mediated bacterial cell-cell interaction.

EseB of *E. tarda* has homology with EspA of *E. coli*. EspA of EPEC can form a sheath-like structure to connect the needle complex with the translocon pore and hence allows translocation of effectors from the bacterial cytosol to the host cell cytosol (17, 33). In addition, EspA filaments act as adhesins in the initial step of biofilm development by EPEC (20), and EHEC exploits EspA filaments for attachment to salad leaves (19). The length of EspA filaments ranges from 32 to 688 nm (34); EseB filaments of *E. tarda* are much longer and can vary in length, ranging from 82 to 3,065 nm (data not shown). As observed in the present study, EseB filaments of *E. tarda* can facilitate bacterial adhesion to an abiotic surface and can facilitate the autoaggregation of and biofilm formation by *E. tarda*. It is therefore considered that EseB and EspA may have multiple functions, in the translocation of effectors, bacterial autoaggregation, and biofilm formation, although *E. tarda* is an intracellular pathogen, and EPEC and EHEC are extracellular pathogens.

The specific role of EseB in bacterial autoaggregation and biofilm formation was validated by anti-EseB antibody treatment. The addition of EseB antibody to *E. tarda* wild-type cultures before autoaggregation reduced autoaggregation in proportion to the amount of antibody added, and the antibody also blocked biofilm formation in a dose-dependent manner. It is possible that the EseB antibody binds to EseB filaments growing on the bacterial surface or blocks the extension of EseB filaments and/or EseB filament-mediated bacterial cell-cell interaction, thus causing decreased autoaggregation of and biofilm formation by *E. tarda* in DMEM. The fact that fewer filaments were detected when cultures were treated with increased amounts of EseB antibody suggests

FIG 2 EseB forms filamentous appendages on the surface of *E. tarda* cells. (A) SEM of *E. tarda* wild-type strain PPD130/91 and the Δ*eseB* strain. Bars, 600 nm. (B) Immuno-TEM images of the *E. tarda* wild-type and Δ*eseB* strains. Bacteria were labeled with anti-EseB antibody and protein A-coated colloidal gold particles conjugated to donkey anti-mouse secondary antibody (10 nm in diameter). Gold particles were distributed along filamentous appendages on *E. tarda* wild-type (black arrows) but not on Δ*eseB* cells. The inset shows enlarged views of the boxed areas. Bars, 200 nm; bar for the inset, 20 nm. (C) Immunofluorescence staining of wild-type and Δ*eseB* cells with antibody against EseB. The fixed bacteria were incubated with anti-EseB antibody, followed by incubation with Alexa 488 donkey anti-mouse secondary antibody. Green filamentous signals were detected in wild-type bacteria but not in Δ*eseB* strain bacteria. Bars, 5 μm.
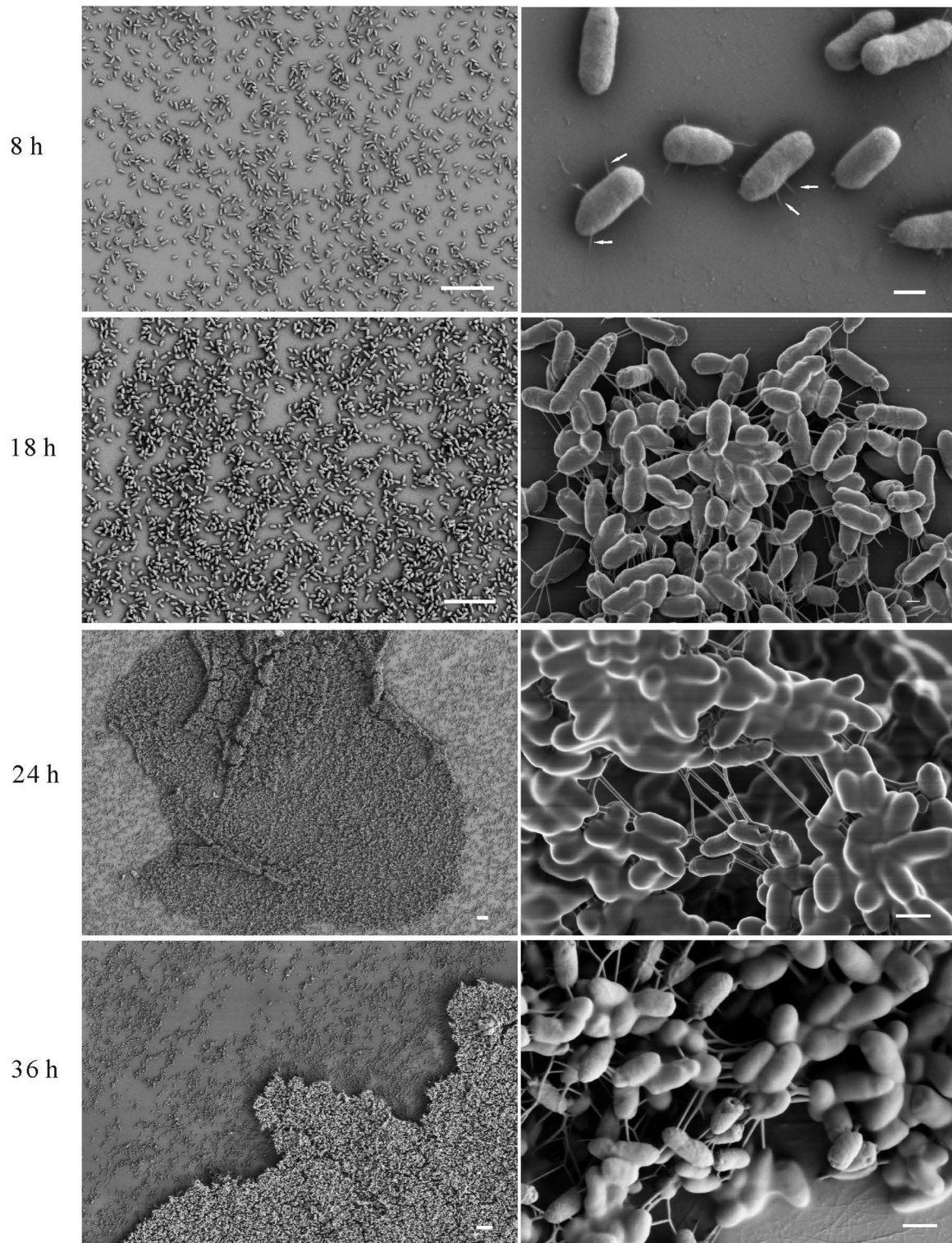
FIG 4 Dynamic analysis of biofilm formation and EseB filaments. At 8 h, 18 h, 24 h, and 36 h postsubculture, *E. tarda* wild-type cells that settled on the coverslips were assayed by SEM. At 8 hps, EseB helps *E. tarda* to attach to the coverslips, as indicated by the white arrows, and at 24 and 36 hps, EseB helps to connect and support *E. tarda* cells. Bars, 10 μm at low magnification (left) and 400 nm at high magnification (right).

that the binding of EseB antibody to growing EseB filaments might destabilize the EseB filaments. On the other hand, mature biofilm is not affected by the EseB antibody added. Together with data from the dynamic analysis of the development of EseB filaments,

autoaggregation, and biofilm formation, we propose that EseB filament-mediated bacterial cell-cell interaction is a prerequisite for autoaggregation of and biofilm formation by *E. tarda* in DMEM. This finding might have wide and important applications
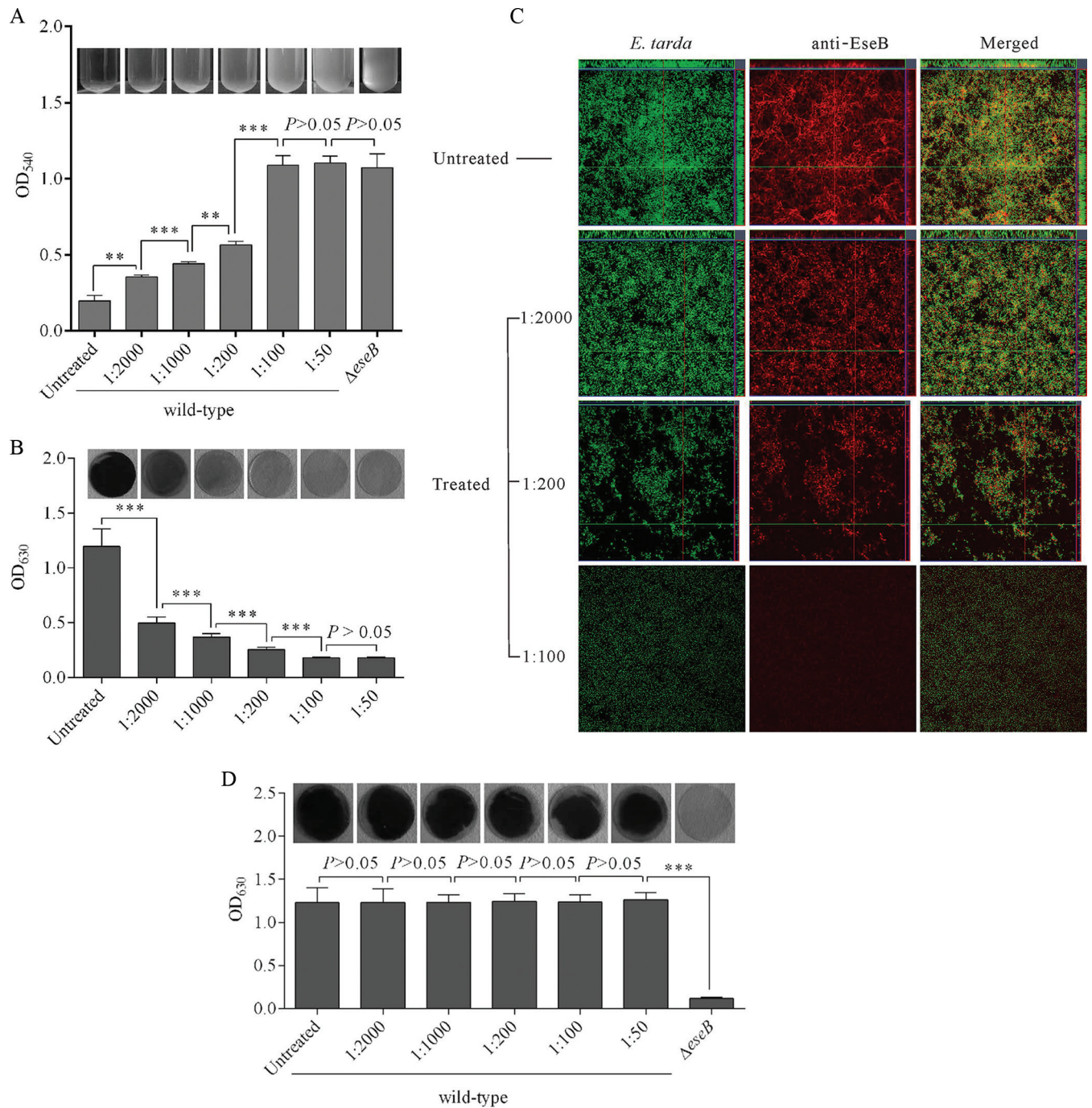
FIG 5 EseB antibody blocks *E. tarda* autoaggregation and biofilm formation. *E. tarda* wild-type cells cultured in DMEM in tubes or 24-well plates were supplemented (Treated) with EseB antibody at 1:2,000, 1:1,000, 1:200, 1:100, and 1:50 dilutions. Naive mouse serum was added to *E. tarda* wild-type cultures at a 1:50 dilution and is labeled Untreated. (A) EseB antibody added at 15 hps inhibits autoaggregation of *E. tarda* cultured in DMEM in a dose-dependent manner, as shown by OD_{540} values of the culture supernatants and images of autoaggregation in glass tubes. ***, $P < 0.001$; **, $P < 0.01$. (B) Biofilm formation by *E. tarda* cultured in DMEM is inversely proportional to the amount of EseB antibody added at 15 hps. Crystal violet staining and quantification of dissolved crystal violet were performed to evaluate the biofilm formation ability in the presence of EseB antibody. ***, $P < 0.001$. (C) Confocal laser scanning microscopy images of top-down views and orthogonal views of filament formation when EseB antibody was added at 15 hps. There were fewer EseB filaments with increasing concentrations of EseB antibody. The amounts of EseB antibody added are indicated for dilutions of no less than 1:100. (D) Mature biofilm formed by *E. tarda* is not influenced by EseB antibody added at 24 hps. The biofilms were examined by crystal violet staining at 4 h post-EseB antibody supplementation. The quality and amount of biofilm formation were revealed by crystal violet staining. ***, $P < 0.001$.

in the prevention of *E. tarda* infection: the EseB protein could be used as a subunit vaccine against *E. tarda* infection.

It has been reported that the motility of bacteria plays an important role in biofilm formation in some species (35, 36). In bacteria, motility is mediated mainly by flagella, which are recognized as the main factor for initial cell-to-surface contact in the attachment stage of EPEC, *S. enterica*, and *Pseudomonas aeruginosa* (37–39). *E. coli* strains lacking flagella or possessing paralyzed flagella are defective in biofilm formation (36, 40). Xu et al. (41) reported previously that flagellum-impaired mutants of *E. tarda* strain H1 exhibited reduced biofilm formation because of decreased attachment to the abiotic polyvinylchloride surface in TSB medium. We found no difference in biofilm formation between wild-type *E. tarda* strain PPD130/91 and its Δ*flhB* flagellar mutant strain grown in DMEM (Fig. 3A). This is not unexpected, as there was no flagellum observed when *E. tarda* was grown in the T3SS-inducing medium DMEM (Fig. 2A). It is likely that under different environmental conditions, *E. tarda* senses different signals to regulate the expression of the corresponding gene to form biofilm.

Filamentous appendages are also observed in other bacteria, for example, outer membrane vesicles (OMVs) on *Myxococcus xanthus* (42), nanofibers on *Streptococcus mutans* (43), and rigid nanowires on *Shewanella oneidensis* (44). Rigid nanowires, which are quite similar to *E. tarda* EseB filaments in morphology and distribution, are electrically conductive in direct response to electron acceptor limitation (44). It would be interesting to know if EseB filaments are also electrically conductive and if this conductivity is related to autoaggregation of and biofilm formation by *E. tarda*.

ACKNOWLEDGMENTS

REFERENCES

1. **Manchanda V, Singh NP, Eideh HK, Shamweel A, Thukral SS.** 2006. Liver abscess caused by *Edwardsiella tarda* biogroup 1 and identification of its epidemiological triad by ribotyping. Indian J Med Microbiol **24:**135–137. http://dx.doi.org/10.4103/0255-0857.25205.

2. **Leung KY, Siame BA, Tenkink BJ, Noort RJ, Mok Y-K.** 2012. *Edwardsiella tarda*—virulence mechanisms of an emerging gastroenteritis pathogen. Microbes Infect **14:**26–34. http://dx.doi.org/10.1016/j.micinf.2011.08.005.

3. **Koido S, Ohkusa T, Kato K, Shimamoto N, Takakura K, Odahara S, Tsukinaga S, Mitobe J, Yukawa T, Kajihara M, Uchiyama K, Arakawa H, Tajiri H.** 2014. *Edwardsiella tarda* superinfection in relapse of ulcerative colitis. J Clin Gastroenterol **48:**191–193. http://dx.doi.org/10.1097/01.mcg.0000437809.46982.df.

4. **Janda JM, Abbott SL, Oshiro L.** 1991. Penetration and replication of *Edwardsiella* spp. in HEp-2 cells. Infect Immun **59:**154–161.

5. **Tan YP, Zheng J, Tung SL, Rosenshine I, Leung KY.** 2005. Role of type III secretion in *Edwardsiella tarda* virulence. Microbiology **151:**2301–2313. http://dx.doi.org/10.1099/mic.0.28005-0.

6. **Okuda J, Kiriyama M, Suzaki E, Kataoka K, Nishibuchi M, Nakai T.** 2009. Characterization of proteins secreted from a type III secretion system of *Edwardsiella tarda* and their roles in macrophage infection. Dis Aquat Organ **84:**115–121. http://dx.doi.org/10.3354/dao02033.

7. **Xie HX, Lu JF, Rolhion N, Holden DW, Nie P, Zhou Y, Yu XJ.** 2014. *Edwardsiella tarda*-induced cytotoxicity depends on its type III secretion system and flagellin. Infect Immun **82:**3436–3445. http://dx.doi.org/10.1128/IAI.01065-13.

8. **Cornelis GR.** 2006. The type III secretion injectisome. Nat Rev Microbiol **4:**811–825. http://dx.doi.org/10.1038/nrmicro1526.

9. **Kudryashev M, Stenta M, Schmelz S, Amstutz M, Wiesand U, Castaño-Díez D, Degiacomi MT, Münnich S, Bleck CK, Kowal J, Diepold A, Heinz DW, Dal Peraro M, Cornelis GR, Stahlberg H.** 2013. In situ structural analysis of the *Yersinia enterocolitica* injectisome. eLife **2:**e00792. http://dx.doi.org/10.7554/eLife.00792.

10. **Fujii T, Cheung M, Blanco A, Kato T, Blocker AJ, Namba K.** 2012. Structure of a type III secretion needle at 7-Å resolution provides insights into its assembly and signaling mechanisms. Proc Natl Acad Sci U S A **109:**4461–4466. http://dx.doi.org/10.1073/pnas.1116126109.

11. **Xie HX, Lu JF, Zhou Y, Yi J, Yu XJ, Leung KY, Nie P.** 2015. Identification and functional characterization of the novel *Edwardsiella tarda* effector EseJ. Infect Immun **83:**1650–1660. http://dx.doi.org/10.1128/IAI.02566-14.

12. **Zheng J, Tung S, Leung KY.** 2005. Regulation of a type III and a putative secretion system in *Edwardsiella tarda* by EsrC is under the control of a two-component system, EsrA-EsrB. Infect Immun **73:**4127–4137. http://dx.doi.org/10.1128/IAI.73.7.4127-4137.2005.

13. **Chakraborty S, Li M, Chatterjee C, Sivaraman J, Leung KY, Mok Y-K.** 2010. Temperature and Mg^{2+} sensing by a novel PhoP-PhoQ two-component system for regulation of virulence in *Edwardsiella tarda*. J Biol Chem **285:**38876–38888. http://dx.doi.org/10.1074/jbc.M110.179150.

14. **Chakraborty S, Sivaraman J, Leung KY, Mok Y-K.** 2011. Two-component PhoB-PhoR regulatory system and ferric uptake regulator sense phosphate and iron to control virulence genes in type III and VI secretion systems of *Edwardsiella tarda*. J Biol Chem **286:**39417–39430. http://dx.doi.org/10.1074/jbc.M111.295188.

15. **Zheng J, Li N, Tan YP, Sivaraman J, Mok Y-K, Mo ZL, Leung KY.** 2007. EscC is a chaperone for the *Edwardsiella tarda* type III secretion system putative translocon components EseB and EseD. Microbiology **153:**1953–1962. http://dx.doi.org/10.1099/mic.0.2006/004952-0.

16. **Wang B, Mo ZL, Xiao P, Li J, Zou YX, Hao B, Li GY.** 2010. EseD, a putative T3SS translocon component of *Edwardsiella tarda*, contributes to virulence in fish and is a candidate for vaccine development. Mar Biotechnol **12:**678–685. http://dx.doi.org/10.1007/s10126-009-9255-5.

17. **Knutton S, Rosenshine I, Pallen MJ, Nisan I, Neves BC, Bain C, Wolff C, Dougan G, Frankel G.** 1998. A novel EspA-associated surface organelle of enteropathogenic *Escherichia coli* involved in protein translocation into epithelial cells. EMBO J **17:**2166–2176. http://dx.doi.org/10.1093/emboj/17.8.2166.

18. **Hartland EL, Daniell SJ, Delahay RM, Neves BC, Wallis T, Shaw RK, Hale C, Knutton S, Frankel G.** 2000. The type III protein translocation system of enteropathogenic *Escherichia coli* involves EspA-EspB protein interactions. Mol Microbiol **35:**1483–1492.

19. **Shaw RK, Berger CN, Feys B, Knutton S, Pallen MJ, Frankel G.** 2008. Enterohemorrhagic *Escherichia coli* exploits EspA filaments for attachment to salad leaves. Appl Environ Microbiol **74:**2908–2914. http://dx.doi.org/10.1128/AEM.02704-07.

20. **Moreira CG, Palmer K, Whiteley M, Sircili MP, Trabulsi LR, Castro AF, Sperandio V.** 2006. Bundle-forming pili and EspA are involved in biofilm formation by enteropathogenic *Escherichia coli*. J Bacteriol **188:**3952–3961. http://dx.doi.org/10.1128/JB.00177-06.

21. **Zimaro T, Thomas L, Marondedze C, Sgro GG, Garofalo CG, Ficarra FA, Gehring C, Ottado J, Gottig N.** 2014. The type III protein secretion system contributes to *Xanthomonas citri* subsp. *citri* biofilm formation. BMC Microbiol **14:**96. http://dx.doi.org/10.1186/1471-2180-14-96.

22. **Jennings ME, Quick LN, Ubol N, Shrom S, Dollahon N, Wilson JW.** 2012. Characterization of *Salmonella* type III secretion hyper-activity which results in biofilm-like cell aggregation. PLoS One **7:**e33080. http://dx.doi.org/10.1371/journal.pone.0033080.

23. **Haussler S, Fuqua C.** 2013. Biofilms 2012: new discoveries and significant wrinkles in a dynamic field. J Bacteriol **195:**2947–2958. http://dx.doi.org/10.1128/JB.00239-13.

24. **Kostakioti M, Hadjifrangiskou M, Hultgren SJ.** 2013. Bacterial biofilms: development, dispersal, and therapeutic strategies in the dawn of the post-antibiotic era. Cold Spring Harb Perspect Med **3:**a010306. http://dx.doi.org/10.1101/cshperspect.a010306.

25. **Drenkard E, Ausubel FM.** 2002. *Pseudomonas* biofilm formation and antibiotic resistance are linked to phenotypic variation. Nature **416:**740–743. http://dx.doi.org/10.1038/416740a.

26. **Flemming HC, Wingender J.** 2010. The biofilm matrix. Nat Rev Microbiol **8**:623–633. http://dx.doi.org/10.1038/nrmicro2415.

27. **Hall-Stoodley L, Costerton JW, Stoodley P.** 2004. Bacterial biofilms: from the natural environment to infectious diseases. Nat Rev Microbiol **2**:95–108. http://dx.doi.org/10.1038/nrmicro821.

28. **Ling SH, Wang XH, Xie L, Lim TM, Leung KY.** 2000. Use of green fluorescent protein (GFP) to study the invasion pathways of *Edwardsiella tarda* in *in vivo* and *in vitro* fish models. Microbiology **146**:7–19.

29. **Khlebnikov A, Skaug T, Keasling JD.** 2002. Modulation of gene expression from the arabinose-inducible *araBAD* promoter. J Ind Microbiol Biotechnol **29**:34–37. http://dx.doi.org/10.1038/sj.jim.7000259.

30. **Valdivia RH, Falkow S.** 1997. Fluorescence-based isolation of bacterial genes expressed within host cells. Science **277**:2007–2011. http://dx.doi.org/10.1126/science.277.5334.2007.

31. **Roine E, Wei W, Yuan J, Nurmiaho-Lassil EL, Kalkkinen N, Romantschuk M, He SY.** 1997. Hrp pilus: an *hrp*-dependent bacterial surface appendage produced by *Pseudomonas syringae* pv. *tomato* DC3000. Proc Natl Acad Sci U S A **94**:3459–3464.

32. **Shaw RK, Daniell S, Ebel F, Frankel G, Knutton S.** 2001. EspA filament-mediated protein translocation into red blood cells. Cell Microbiol **3**:213–222. http://dx.doi.org/10.1046/j.1462-5822.2001.00105.x.

33. **Daniell SJ, Kocsis E, Morris E, Knutton S, Booy FP, Frankel G.** 2003. 3D structure of EspA filaments from enteropathogenic *Escherichia coli*. Mol Microbiol **49**:301–308. http://dx.doi.org/10.1046/j.1365-2958.2003.03555.x.

34. **Sekiya K, Ohishi M, Ogino T, Tamano K, Sasakawa C, Abe A.** 2001. Supermolecular structure of the enteropathogenic *Escherichia coli* type III secretion system and its direct interaction with the EspA-sheath-like structure. Proc Natl Acad Sci U S A **98**:11638–11643. http://dx.doi.org/10.1073/pnas.191378598.

35. **Meshcheryakov VA, Barker CS, Kostyukova AS, Samatey FA.** 2013. Function of FlhB, a membrane protein implicated in the bacterial flagellar type III secretion system. PLoS One **8**:e68384. http://dx.doi.org/10.1371/journal.pone.0068384.

36. **Wood TK, González Barrios AF, Herzberg M, Lee J.** 2006. Motility influences biofilm architecture in *Escherichia coli*. Appl Microbiol Biotechnol **72**:361–367. http://dx.doi.org/10.1007/s00253-005-0263-8.

37. **Rashid MH, Kornberg A.** 2000. Inorganic polyphosphate is needed for swimming, swarming, and twitching motilities of *Pseudomonas aeruginosa*. Proc Natl Acad Sci U S A **97**:4885–4890. http://dx.doi.org/10.1073/pnas.060030097.

38. **Girón JA, Torres AG, Freer E, Kaper JB.** 2002. The flagella of enteropathogenic *Escherichia coli* mediate adherence to epithelial cells. Mol Microbiol **44**:361–379. http://dx.doi.org/10.1046/j.1365-2958.2002.02899.x.

39. **Crawford RW, Reeve KE, Gunn JS.** 2010. Flagellated but not hyperfimbriated *Salmonella enterica* serovar Typhimurium attaches to and forms biofilms on cholesterol-coated surfaces. J Bacteriol **192**:2981–2990. http://dx.doi.org/10.1128/JB.01620-09.

40. **Houry A, Briandet R, Aymerich S, Gohar M.** 2010. Involvement of motility and flagella in *Bacillus cereus* biofilm formation. Microbiology **156**:1009–1018. http://dx.doi.org/10.1099/mic.0.034827-0.

41. **Xu T, Su Y, Xu Y, He Y, Wang B, Dong X, Li Y, Zhang XH.** 2014. Mutations of flagellar genes *fliC12*, *fliA* and *flhDC* of *Edwardsiella tarda* attenuated bacterial motility, biofilm formation and virulence to fish. J Appl Microbiol **116**:236–244. http://dx.doi.org/10.1111/jam.12357.

42. **Remis JP, Wei D, Gorur A, Zemla M, Haraga J, Allen S, Witkowska HE, Costerton JW, Berleman JE, Auer M.** 2014. Bacterial social networks: structure and composition of *Myxococcus xanthus* outer membrane vesicle chains. Environ Microbiol **16**:598–610. http://dx.doi.org/10.1111/1462-2920.12187.

43. **Liao S, Klein MI, Heim KP, Fan Y, Bitoun JP, Ahn SJ, Burne RA, Koo H, Brady LJ, Wen ZT.** 2014. *Streptococcus mutans* extracellular DNA is upregulated during growth in biofilms, actively released via membrane vesicles, and influenced by components of the protein secretion machinery. J Bacteriol **196**:2355–2366. http://dx.doi.org/10.1128/JB.01493-14.

44. **Gorby YA, Yanina S, McLean JS, Rosso KM, Moyles D, Dohnalkova A, Beveridge TJ, Chang IS, Kim BH, Kim KS, Culley DE, Reed SB, Romine MF, Saffarini DA, Hill EA, Shi L, Elias DA, Kennedy DW, Pinchuk G, Watanabe K, Ishii S, Logan B, Nealson KH, Fredrickson JK.** 2006. Electrically conductive bacterial nanowires produced by *Shewanella oneidensis* strain MR-1 and other microorganisms. Proc Natl Acad Sci U S A **103**:11358–11363. http://dx.doi.org/10.1073/pnas.0604517103.